

# Synthesis and Physical Properties of $Mn_xNbS_2$

K. Miwa, H. Ikuta, H. Hinode, T. Uchida, and M. Wakihara<sup>1</sup>

*Department of Chemical Engineering, Tokyo Institute of Technology, 2-12-1 Ookayama, Meguro-ku, Tokyo 152 Japan*

Received January 17, 1996; in revised form May 21, 1996; accepted May 28, 1996

The intercalation compounds of the Mn–Nb–S system were synthesized from the elements at 1000°C in evacuated quartz ampoules. The single phase region was obtained as  $0.19 \leq x \leq 0.52$  in  $Mn_xNbS_2$ . The hexagonal  $a$  parameter increased with increasing Mn composition from  $x = 0.19$  to 0.45 and then suddenly decreased from  $x = 0.45$  to 0.52. The  $c$  parameter increased monotonically with increasing  $x$ . The magnetic susceptibility of  $Mn_xNbS_2$  obeyed a Curie–Weiss law, and the Weiss temperature  $\theta$  decreased with increasing  $x$  and changed from positive to negative at  $x \sim 0.4$ . The temperature dependence of electrical resistivity showed metallic behavior. The magnetic susceptibility measurements suggested the high-spin state of  $Mn^{2+}$ . © 1996 Academic Press, Inc.

## 1. INTRODUCTION

Almost all the transition-metal dichalcogenides,  $MX_2$ , crystallize in a characteristic layered structure where  $M$  are transition metal atoms of group 4 (Ti, Zr, Hf), group 5 (V, Nb, Ta), and group 6 (Cr, Mo, W), and  $X$  are chalcogen atoms of group 16 (S, Se, Te). Two-dimensional slabs are formed by two layers of close-packed chalcogenide atoms sandwiching one metal layer between them. Then these  $MX_2$  slabs are stacked with just van der Waals gaps between the slabs. A variety of atoms or molecules can be intercalated in the van der Waals gap.

Niobium disulfide  $NbS_2$  has been paid attention because of characteristic optical (1, 2), magnetic properties (3–5), superconductivity (3, 6, 7), and super structures including polytype (1). It has been considered that these interesting properties are mainly caused by a metal–metal interaction of intra-metal layers. The structure of  $NbS_2$  belongs to a hexagonal system, and the S–Nb–S sandwich layers pile along the  $c$  axis. In the octahedral holes of the van der Waals gaps of  $NbS_2$  transition metals such as Ti, V, Cr, Mn, Fe, Co, and Ni can be accommodated. However, such intercalation compounds,  $M_xNbS_2$ , have been reported only for the symmetrical compositions of  $M$ , i.e.,  $x = \frac{1}{2}$ ,  $\frac{1}{3}$ , and  $\frac{1}{4}$ , and little information has been given on the single

phase region, or on the compositional variations of physical properties of  $M_xNbS_2$  (4, 5). In our laboratory, we have investigated the Fe–Nb–S system, and the Mössbauer studies of  $(Fe_yNb_{1-y})_{1+x}S_2$  have been carried out (8).

Since, on the Mn–NbS<sub>2</sub> intercalation compounds, the magnetic susceptibility (9–12) and the electrical resistivity (13) only for  $Mn_{1/3}NbS_2$  and  $Mn_{1/4}NbS_2$  have been reported in the literature, the single phase region of  $Mn_xNbS_2$  and compositional variation of the physical properties in a wide range of  $x$  were studied in the present paper.

## 2. EXPERIMENTAL

### *Sample Preparation*

The intercalation compounds  $Mn_xNbS_2$  were prepared by mixing Mn powder (Soekawa Chemicals Co., 99.98%), Nb powder (Soekawa Chemicals Co., 99.9%), and crystalline S (Soekawa Chemicals Co., 99.9999%). They were mixed with a desired ratio, pressed into a pellet and sealed in an evacuated quartz ampoule. The pellet was heated first at 400°C for 1 day and then at 1000°C for 1 week. The obtained sample was ground, sealed again, heated at 1000°C for another 1 week, and quenched in ice water. The phase identification and the evaluation of the lattice parameters of the samples were carried out by powder X-ray diffractometry using  $CuK\alpha$  radiation obtained from a high-power X-ray generator (Rotaflex RU-200A, Rigaku Co. Ltd.).

### *Physical Property Measurements*

The magnetic susceptibility was measured using the SQUID method (Quantum Design MPMS-5A) in the temperature range 4.2–300 K under the static field of 1000 G. The electrical resistivity measurements on the pelletized samples (5 mm diameter  $\times$  8 mm thickness) were performed using the standard dc four-probe technique under  $H_2$  atmosphere in the temperature range 90–300 K.

## 3. RESULTS AND DISCUSSION

From the powder X-ray diffraction patterns of  $Mn_xNbS_2$ , the single phase region with a  $2Ha$ – $NbS_2$  struc-

<sup>1</sup> To whom correspondence should be addressed.

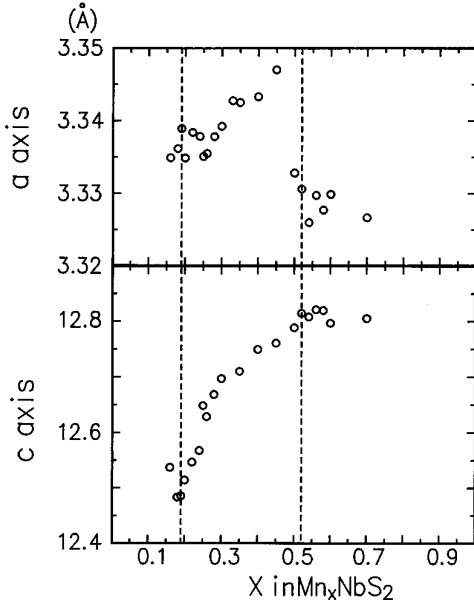


FIG. 1. Plot of lattice parameters  $a$  and  $c$  of  $\text{Mn}_x\text{NbS}_2$ .

ture was determined to be  $0.19 \leq x \leq 0.52$ . Mixed phases of 2Ha-type and 3R-type were observed in  $x < 0.19$  and unknown impurities peaks appeared in  $x > 0.52$ . The relationship between the manganese composition  $x$  and the hexagonal lattice parameters  $a$  and  $c$  is shown in Fig. 1. The  $a$  parameter increased with increasing  $x$  from  $x = 0.19$  to 0.45 and then suddenly decreased from  $x = 0.45$  to 0.52. In contrast, the  $c$  parameter increased monotonically with an increase of the manganese composition  $x$ . The manganese ions intercalated to the van der Waals gap and lengthened the lattice in the direction of the  $c$  axis.

Figure 2 shows the temperature dependence of magnetic susceptibility. In all the samples the temperature depen-

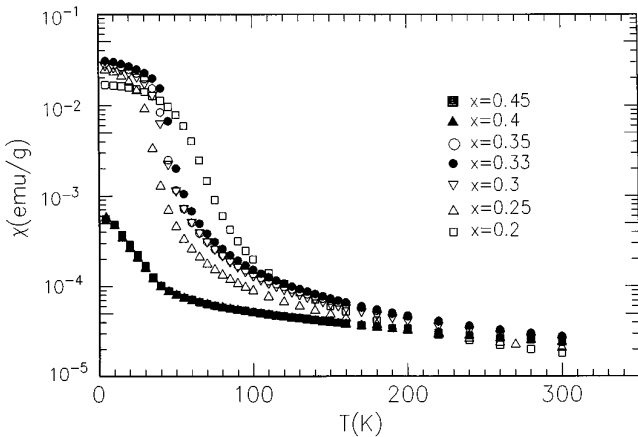


FIG. 2. Temperature dependence of magnetic susceptibility of  $\text{Mn}_x\text{NbS}_2$ .

TABLE 1  
Magnetic Parameters of  $\text{Mn}_x\text{NbS}_2$

Composition $x$	$\theta$ (K)	$C(10^{-3} \text{ emu/g})$	$p_{\text{eff}}(\mu_B)$	$S$
0.2	73.41	5.43	6.04	2.56
0.25	38.31	5.75	5.61	2.35
0.3	49.22	6.84	5.62	2.36
0.33	52.54	7.44	5.62	2.35
0.35	43.49	8.38	5.81	2.45
0.4	-63.1	7.91	5.32	2.21
0.45	-80.74	9.62	5.58	2.33

dence of magnetic susceptibility obeyed a Curie–Weiss law described by

$$\chi = \chi_0 + \frac{C_{\text{mol}}}{T - \theta},$$

where  $\chi_0$  is a temperature-independent term,  $C_{\text{mol}}$  a molar Curie constant, and  $\theta$  a Weiss temperature. The relationship between temperature and inverse magnetic susceptibility is shown in Fig. 3. The values of  $C_{\text{mol}}$  and  $\theta$  in Table 1 were obtained by using a least squares refinement.  $\theta$  decreased with increasing  $x$  and changed from positive to negative at  $x \sim 0.4$ , suggesting that the magnetic interactions changed from ferromagnetic to antiferromagnetic at  $x \sim 0.4$ .  $\chi_0$  is influenced by diamagnetism for electrons around the atomic nucleus and Pauli paramagnetism for conduction electrons. Though  $\chi_0$  is on the order of  $10^{-6}$  emu/g, it was impossible to estimate its exact value.  $P_{\text{eff}}$  is an effective Bohr magneton per a Mn atom calculated by using the value of  $C_{\text{mol}}$ . Values of  $S$  obtained by assuming that only spins contribute to  $C_{\text{mol}}$  showed that the valence of manganese is expected to be high spin state of  $\text{Mn}^{2+}$ .

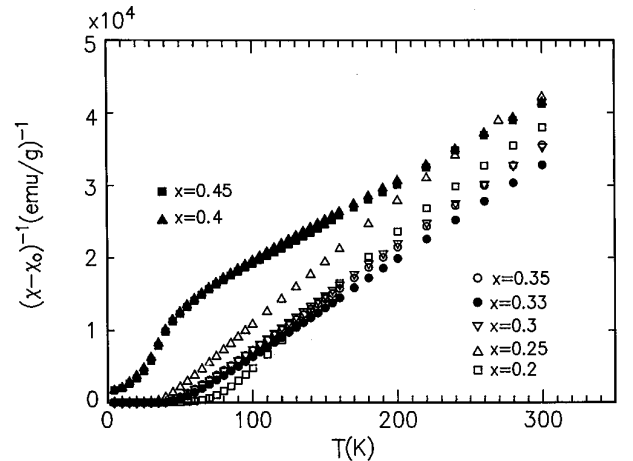


FIG. 3. Inverse magnetic susceptibility vs temperature of  $\text{Mn}_x\text{NbS}_2$ .

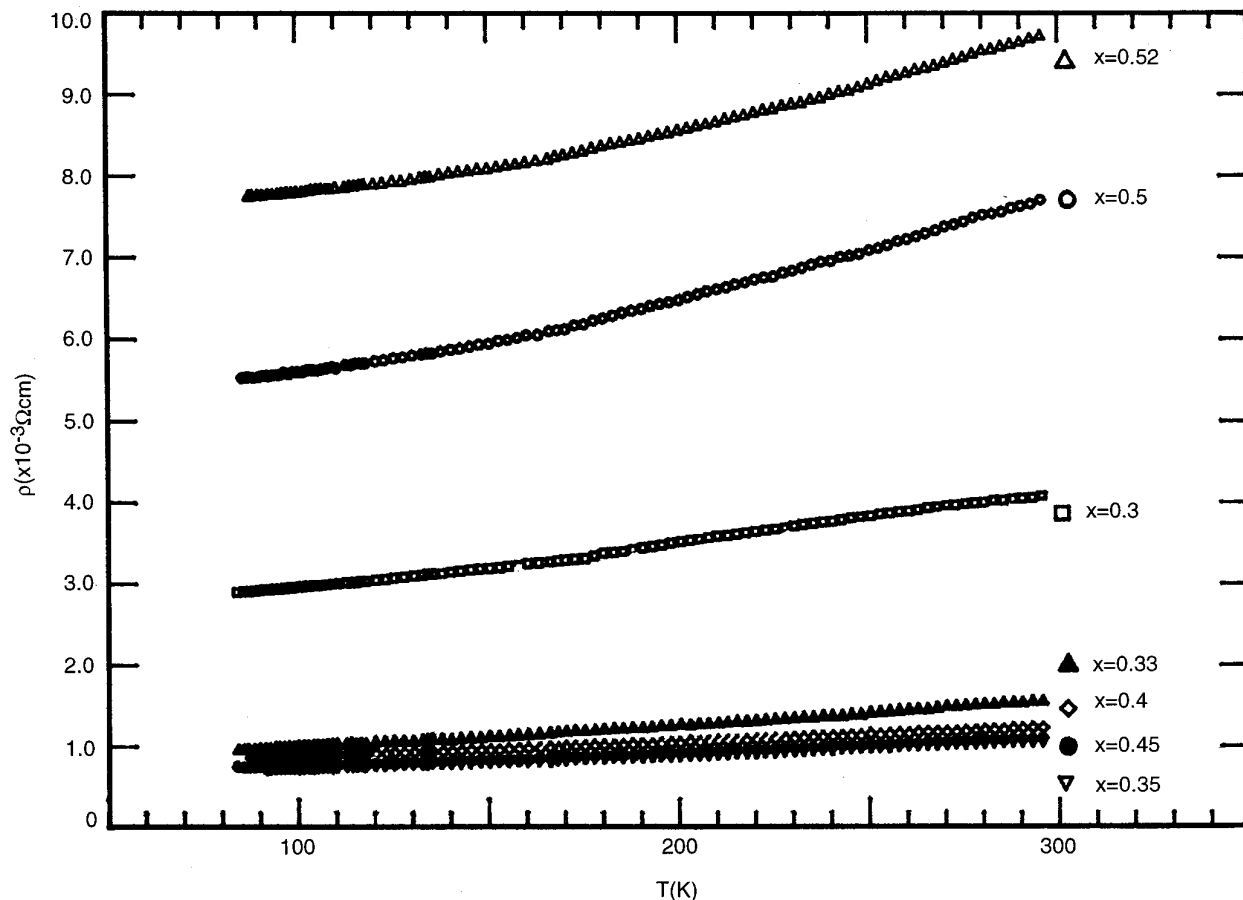


FIG. 4. Electrical resistivity of  $Mn_xNbS_2$ .

The electrical resistivity for various compositions of  $x$  against temperature is shown in Fig. 4. Well sintered pellets were obtained for  $Mn_xNbS_2$  with  $x \geq 0.3$ , while the pellets of the samples with  $x < 0.3$  poorly sintered. Therefore, we plotted the data of  $x \geq 0.3$  in Figs. 4 and 5. The resistivity increased with increasing temperature in all the samples, which indicated metallic behavior. Figure 5 shows the composition dependence of resistivity at room temperature. At first the resistivity decreased with an increase in the composition  $x$  and then suddenly increased at  $x \sim 0.5$ . This behavior can be explained by the rigid band model of  $NbS_2$  (14). Figure 6 shows the band structure of  $NbS_2$ . The  $d_{z2}$  band of  $NbS_2$  can accommodate one electron because the Fermi level in the host  $NbS_2$  lies in the middle of the  $d_{z2}$  band. In the range  $0.3 < x < 0.45$ , free electrons increased by intercalation of manganese, and this resulted in the reduction of the resistivity. The sudden increase in the resistivity in  $x \geq 0.45$  will be ascribed to the idea that the  $d_{z2}$  band is fully filled with the electron donated as the result of Mn intercalation. This, in turn, suggests that manganese is divalent. This supposition agrees with

the result of the present magnetic susceptibility measurement.

It is noteworthy that the structural change, i.e., the change in the  $a$  parameter, is correlated to the change in the resistivity at room temperature.

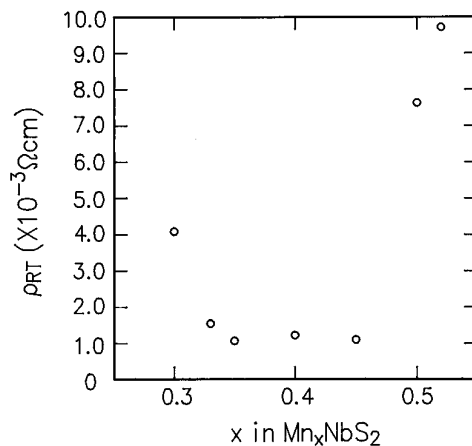


FIG. 5. Room temperature resistivity of  $Mn_xNbS_2$ .

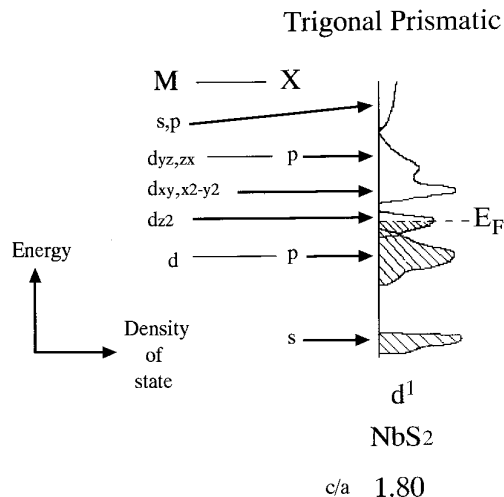


FIG. 6. Band structure of  $NbS_2$ .

#### 4. CONCLUSIONS

(i) The manganese composition in the single phase of  $Mn_xNbS_2$  was  $0.19 \leq x \leq 0.52$ . The hexagonal lattice  $a$  parameter increased until  $x = 0.45$  and suddenly decreased from  $x = 0.45$  to  $0.52$ . The  $c$  parameter increased monotonically with an increase in the manganese composition  $x$ .

(ii) Magnetic susceptibility obeyed a Curie-Weiss law, ferromagnetic behavior was observed in  $x \leq 0.35$ , and antiferromagnetic behavior was observed in  $x \geq 0.4$ . Values

of  $S$  showed that the valence of manganese is expected to be the high spin state of  $Mn^{2+}$ .

(iii) In the electrical resistivity measurements, metallic behavior was observed in all the samples.

(iv) The rigid band model could explain that the valence of the manganese ion is +2.

#### ACKNOWLEDGMENTS

We express our gratitude to Professor Enoki (Tokyo Institute of Technology) for measuring the magnetic susceptibility.

#### REFERENCES

1. J. A. Wilson and A. D. Yoffe, *Adv. Phys.* **18**, 193 (1969).
2. Z. M. Li, B. Bergersen, P. Palffy-Muhoray, and D. Beigie, *Can. J. Phys.* **66**, 228 (1988).
3. W. G. Fisher and M. J. Sienko, *Inorg. Chem.* **19**, 39 (1980).
4. F. Hulliger and E. Pobitschka, *J. Solid State Chem.* **1**, 117 (1970).
5. J. M. van den Berg and P. Cossee, *Inorg. Chim. Acta* **2**, 143 (1968).
6. M. Ikebe and Y. Muto, *Synthetic Met.* **5**, 229 (1983).
7. M. H. Van Maaren and H. B. Harland, *Phys. Lett. A* **29**, 571 (1969).
8. M. Wakihara, H. Hinode, M. Abe, and M. Taniguchi, *J. Solid State Chem.* **36**, 339 (1981).
9. F. Jellinek, *Ark. Kemi (Sweden)* **20**, 447 (1963).
10. S. S. P. Parkin and R. H. Friend, *Physica B* **99**, 219 (1980).
11. K. Anzenhofer, J. M. Van Den Berg, P. Cossee, and J. N. Helle, *J. Phys. Chem. Solids* **31**, 1057 (1970).
12. B. Van Laar, H. M. Rietveld, and D. J. W. Ijdo, *J. Solid State Chem.* **3**, 154 (1971).
13. Y. Onuki, K. Ina, T. Hirai, and T. Komatsubara, *J. Phys. Soc. Japan* **55**, 347 (1986).
14. R. H. Friend and A. D. Yoffe, *Adv. Phys.* **36**, 1 (1987).